https://doi.org/10.5194/egusphere-2025-5838
Preprint. Discussion started: 26 January 2026
© Author(s) 2026. CC BY 4.0 License.

ITMSL: an improved ice thickness inversion model integrating basal sliding dynamics for High Mountain Asia (v1.0.0)

Xiaoguang Pang[1,2], Liming Jiang[2,3], Yuxuan Wu[2], Xi Lu[2], Yi Liu[2,3], Xiaoen Li[2,3], Tingting Yao[1]

[1]College of Information Science and Engineering, Henan University of Technology, Henan, China
[2]State Key Laboratory of Precision Geodesy, Innovation Academy for Precision Measurement Science and Technology, Chinese Academy of Sciences, Wuhan 430077, China
[3]College of Earth and Planetary Science, University of Chinese Academy of Sciences, Beijing 100049, China

Correspondence: Liming Jiang (jlm@whigg.ac.cn)

Highlights.

1. We develop the Ice Thickness Model considering Sliding Law (ITMSL), an enhanced laminar-flow inversion with higher accuracy and physical realism.
2. ITMSL enables automated joint inversion of glacier thickness and basal sliding.
3. ITMSL improves ice-thickness accuracy by at least 16% over traditional ratio-assumption methods in High Mountain Asia (HMA).

Abstract. Glacier thickness plays a fundamental role in understanding ice dynamics, hydrological resources, and glacial hazards. Current ice thickness inversion primarily uses laminar flow theory constrained by geometric, topographic, and ice flow characteristics. However, these approaches oversimplify basal sliding parameterization, leading to substantial uncertainties and significant biases in thickness estimates. Here, we present an improved ice thickness estimation approach through the integration of basal sliding dynamics into laminar flow theory, termed the Ice Thickness Model considering Sliding Law (ITMSL). We apply and evaluate the model's performance and limitations across High Mountain Asia (HMA), a region characterized by complex topography and data scarcity. The model enables automated large-scale ice thickness reconstruction while simultaneously determining basal sliding velocities and subglacial topography. Validation against ground-penetrating radar (GPR) measurements on 16 glaciers shows that, compared to existing laminar flow-based models GV14 (Gantayat et al., 2014) and GV22 (Millan et al., 2022), ITMSL achieves better performance, with accuracy improved by 16.2% and 28.9%, respectively. This study has demonstrated that ITMSL provides

https://doi.org/10.5194/egusphere-2025-5838
Preprint. Discussion started: 26 January 2026
© Author(s) 2026. CC BY 4.0 License.

an improvement over previous methods, offering new insights for ice thickness modeling and its application in data-sparse high mountain regions.

1 Introduction

High Mountain Asia (HMA), encompassing the Qinghai-Tibet Plateau and surrounding regions including the Karakoram, Pamir, Himalayas, and Tien Shan (Yao et al., 2012; Chen et al., 2022; Fan et al., 2022; Wang et al., 2023), represents the most densely glacierized region outside the polar realms (Farinotti et al., 2019; Wang et al., 2023). HMA glaciers hold an estimated volume of 7000 km^3, constituting the critical "Asian Water Tower"(Miles et al., 2021). This region serves as the headwater for major Asian rivers, including the Yangtze, Yellow, and Brahmaputra (Brun et al., 2017). Glacier meltwater provides a vital, continuous water source for millions downstream, sustaining agriculture and domestic use—particularly in arid northwestern China (Kraaijenbrink et al., 2017; Miles et al., 2021; Li et al., 2022; Bolch et al., 2012). Glacier thickness distribution is therefore a key parameter for managing freshwater resources and projecting future glacier evolution (Fang et al., 2024; Lannutti et al., 2024; Robel et al., 2024; Wang et al., 2024). Consequently, advancing ice thickness models and large-scale glacier volume estimates is essential for regional water resource management and glacier change prediction.

Glacier thickness has been estimated using both in situ measurements and modeling approaches. These include field techniques such as ground-penetrating radar (GPR), drilling, geomagnetic soundings, and seismic surveys (Wang et al., 2016; Van Tricht et al., 2021; Veitch et al., 2021; Liang and Tian, 2022), as well as physical models (Farinotti et al., 2017; Farinotti et al., 2019; Millan et al., 2022) and volume-area (V-A) scaling (Radić and Hock, 2010; Grinsted, 2013). However, in situ methods remain limited due to harsh high-altitude environments and logistical difficulties. Many glaciers are remote, making substantial manpower and material resources (Wu et al., 2020; Li et al., 2022; Pang et al., 2023). While widely used, V-A scaling cannot resolve the spatial distribution of glacier thickness (Bahr et al., 2015; Li et al., 2022; Liang and Tian, 2022; Pang et al., 2023). To date, approximately 20 ice thickness models have been proposed, including H-F, OGGM, GlabTop2, and models based on laminar flow theory (Huss and Farinotti, 2012; Frey et al., 2014; Gantayat et al., 2014; Farinotti et al., 2019; Maussion et al., 2019; Millan et al., 2022). The laminar flow-based ice thickness model estimates ice thickness by assuming that the basal sliding is constant (Gantayat et al., 2014; Wu et al., 2020; Millan et al., 2022). Examples

https://doi.org/10.5194/egusphere-2025-5838
Preprint. Discussion started: 26 January 2026
© Author(s) 2026. CC BY 4.0 License.

include: assuming a fixed sliding ratio of 25% (hereafter GV14) (Gantayat et al., 2014), deriving the ratio from the relationship between slope and surface velocity (hereafter GV22) (Millan et al., 2022), or assuming zero basal sliding during winter (Wu et al., 2020). However, basal sliding is a complex process influenced by subglacial topography, basal shear stress, and ice overburden pressure (Weertman, 1957; Schoof, 2005; Cuffey and Paterson, 2010; Zoet and Iverson, 2020; Helanow et al., 2021), the ratio of basal sliding to surface velocity exhibits significant spatial and temporal variability within glaciers, with observed values ranging widely from 0.03 to 1 (Engelhardt and Kamb, 1998; Cuffey and Paterson, 2010; Echelmeyer and Zhongxiang, 1987). Therefore, accurately accounting for basal sliding dynamics is essential to improve the accuracy of ice thickness estimation within laminar flow theory.

Basal sliding laws are commonly employed in glacier dynamics to simulate this process (Zekollari et al., 2022; Schoof, 2005; Joughin et al., 2019; Zoet and Iverson, 2020). These laws typically assume the glacier rests on hard bedrock (Weertman, 1957; Cuffey and Paterson, 2010), with basal motion governed by basal shear stress, effective pressure, and bed roughness (Budd et al., 1979; Schoof, 2005; O. et al., 2007; Woodard et al., 2022). Compared with traditional simple assumptions, these laws more accurately capture the spatial characteristics of basal sliding and its physical relationships with other variables. Here, we address limitations in glacier thickness inversion under laminar flow theory by developing a novel model (ITMSL) that integrates basal sliding laws. This model is driven by glacier topography and surface velocity. The parameters and accuracy of inversion results was validated and assessed against in situ observations. We applied ITMSL to 16 glaciers across HMA, comparing its performance against two established models (GV14 and GV22). In addition, we evaluated the influence of different DEMs on model performance to identify optimal datasets for glacier thickness estimation in HMA.

In the subsequent sections, we will present the theoretical (Section 2), implementation workflow of the model (Section 3), evaluate its inversion results against existing ice thickness models (Section 4), discuss certain limitations and possible improvements (Section 5), and conclude with a summary (Section 6).

2 Methods

The following section details the datasets used to drive the model and the theoretical derivation process underlying its construction.

https://doi.org/10.5194/egusphere-2025-5838
Preprint. Discussion started: 26 January 2026
© Author(s) 2026. CC BY 4.0 License.

2.1 Datasets

Glaciers in HMA are influenced by the Indian monsoon, westerlies, and East Asian monsoon (Bolch et al., 2012; Yao et al., 2012). These climatic regimes drive pronounced spatial heterogeneity in glacier distribution, mass balance, and dynamic (Hugonnet et al., 2021; Miles et al., 2021; Millan et al., 2022; Wang et al., 2023). For this study, we selected 16 glaciers spreading across the Tian Shan (7 glaciers), Himalayas (1 glacier), Qilian Shan (2 glaciers), and Karakoram (6 glaciers) (Figure 1). The sample exhibit significant diversity in area, width, and surface velocity. Notably, one glacier covers less than 1 km^2, while 9 exceed 5 km^2 (Table 1). The Urumqi No.1 Glacier (Tian Shan) bifurcated into eastern and western branches in 1993 (Wang et al., 2016); we analyze these branches as a single glacier.

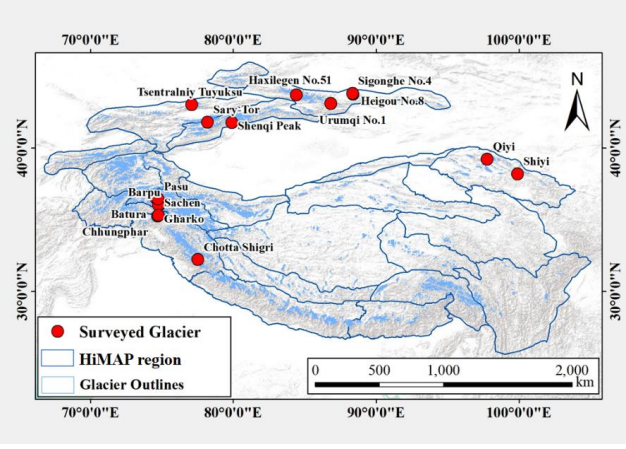

Figure 1: Distribution of HMA glaciers and the location of selected glaciers.

This study utilized glacier outlines from the Randolph Glacier Inventory version 6.0 (RGI 6.0; https://www.glims.org/RGI/) (Pfeffer et al., 2014). Topographic features essential for ice thickness inversion—including surface slope and elevation—were derived from the Copernicus DEM GLOB-30 (hereafter COPDEM30; https://registry.opendata.aws/copernicus-dem). COPDEM30 provides near-global coverage at 30m resolution, generated through reprocessing of WorldDEMTM data acquired between 2011 and 2015. The reprocessing involved resampling, void filling, and replacement of anomalous elevation values (Becek et al., 2016; González-Moradas and Viveen, 2020; Hawker et al., 2022; Li et al., 2022). The Copernicus DEM exhibits an absolute vertical accuracy of 4 m and relative vertical accuracy of 2 m (Hawker et al., 2022). For computational efficiency in ice thickness modeling, COPDEM30 data were resampled to 50m resolution.

https://doi.org/10.5194/egusphere-2025-5838
Preprint. Discussion started: 26 January 2026
© Author(s) 2026. CC BY 4.0 License.

Ice thickness models based on laminar flow theory estimate glacier thickness using ice motion characteristics (Gantayat et al., 2014; Millan et al., 2022). This study utilizes glacier surface velocities from Millan et al, (2022), who derived ice flow velocities for 2017-2018 by applying sub-pixel correlation techniques to remote sensing imagery (Millan et al., 2019; Millan et al., 2022). The dataset features a spatial resolution of 50 m with a reported velocity uncertainty of 10 m/yr.

To evaluate model-derived ice thickness accuracy, we collected GPR measurements from 16 glaciers. Data sources include the Glacier Thickness Database version 3 (GlaThiDa v3), maintained by the Global Terrestrial Network for Glaciers (GTN-G) through the World Glacier Monitoring Service (WGMS; https://wgms.ch/), as well as published studies (Azam et al., 2012; Welty et al., 2020; Farinotti et al., 2021). GlaThiDa represents a global compilation of ice thickness measurements obtained through GPR, drilling, and seismic methods (Welty et al., 2020). For our study glaciers, temporal inconsistencies between ice thickness measurements and DEM/outline acquisition dates are considered negligible (Li et al., 2022).

Table 1: Glaciers from RGI 6.0, survey years, and GPR data sources.

Glacier (abbreviation)	Area (km^2)	Elevation extent (m)	GPR Survey Year	GPR source
Barpu (BARP)	104.952	2810～7291	2015~2018	(Zou et al., 2021)
Batura (BATU)	311.419	2578～7772	2015~2018	
Chhungphar (CHHU)	15.136	2934～6760	2015~2018	
Gharko (GHAR)	30.318	3089～6774	2015~2018	
Pasu (PASU)	62.145	2571～7605	2015~2018	
Sachen (SACH)	10.307	3387～5549	2015~2018	
Haxilegen No.51 (HXLG)	1.099	3481～3907	2010	(Welty et al., 2020)
Heigou No.8 (HEIG)	6.074	3380～5206	2009	
Urumqi No.1 (URUM)	1.579	3747～4463	2014	
Qiyi (QIYI)	2.530	4299～5133	1980	
Sary-Tor (SARY)	2.927	3859～4740	2013	
Shenqi Peak (SHQI)	6.591	3770～5951	2008	
Shiyi (SHIY)	0.495	4327～4772	2010	

https://doi.org/10.5194/egusphere-2025-5838
Preprint. Discussion started: 26 January 2026
© Author(s) 2026. CC BY 4.0 License.

Sigonghe No.4 (SIGH)	2.641	3624～4334	2009	
Tsentralniy Tuyuksu (TSTU)	2.838	3420～4207	2013	
Chhota Shigri (CTSG)	13.463	4268～5755	2009	(Azam et al., 2012)

2.2 Ice thickness model considering basal sliding law (ITMSL)

Laminar flow theory is a fundamental framework in glacier dynamics (Cuffey and Paterson, 2010). It describes the glacier surface velocity as the sum of ice deformation and basal sliding (Gantayat et al., 2014; Wu et al., 2020):

$$u_s = u_b + \frac{2A}{n+1}\tau_b^n H \quad (1)$$

where u_s and u_b (m/s) are the surface and basal sliding velocity, respectively. n is Glen's flow law exponent, typically assumed to be 3. A is the creep parameter, dependent on ice temperature, fabric, grain size, and water content. Here we use $A = 2.4 \times 10^{-24}\mathrm{Pa}^{-3}\mathrm{s}^{-1}$ (Cuffey and Paterson, 2010; Gantayat et al., 2014). H (m) is the ice thickness. τ_b (Pa) is the basal shear stress, calculated as (Li et al., 2012):

$$\tau_b = f\rho g H sin\alpha \quad (2)$$

where ρ is the ice density, taken as a constant $900\ \mathrm{kg \cdot m^{-3}}$, g is the acceleration due to gravity ($9.8\ \mathrm{m \cdot s^{-2}}$), α is the glacier surface slope (Farinotti et al., 2017; Farinotti et al., 2019). f is the valley shape factor, a dimensionless parameter accounting for the influence of glacier cross-sectional geometry on the relationship between driving stress and basal shear stress (Li et al., 2012; Ramsankaran et al., 2018). f is estimated using glacier width (w) and ice thickness (H):

$$f = \frac{2}{\pi} arctan(\frac{w}{2H}) \quad (3)$$

When laminar flow theory is used to estimate glacier thickness, assumptions are made regarding the ratio of u_b to u_s (Gantayat et al., 2014; Millan et al., 2022).

There are three types of basal sliding laws for glaciers (Weertman, 1957; Budd et al., 1979; Schoof, 2005). Weertman derived a basal sliding law by modelling the glacier bed as uniformly distributed regular cubic obstacles (Weertman, 1957). This law incorporates two key mechanisms: pressure melting and enhanced ice creep, establishing a nonlinear relationship between basal sliding velocity, basal shear stress, and ice bed roughness (Weertman, 1957). However, Weertman's formulation neglects the

https://doi.org/10.5194/egusphere-2025-5838
Preprint. Discussion started: 26 January 2026
© Author(s) 2026. CC BY 4.0 License.

influence of subglacial water content variations on sliding. To address this limitation, Budd introduced a sliding law accounting for basal cavity evolution, through it retains a power-law form (Budd et al., 1979; Fowler and Frank, 1981). Crucially, basal shear stress increases with sliding velocity until reaching a limit controlled by subglacial hydrology (Iken, 1981). As water pressure rises, basal drag approaches a maximum value determined by the maximum bed slope (Schoof, 2005; O. et al., 2007; Zoet and Iverson, 2020; Helanow et al., 2021; Gilbert et al., 2023). To ensure the sliding law accurately represents this complex interaction between water pressure, shear stress, and dynamics, we implement the following formulation:

$$\frac{\tau_b}{N} = C\left(\frac{u_b}{u_b + A_s C^n N^n}\right)^{1/n} \quad (4)$$

where N (Pa) is the effective pressure; $C = 0.84 \pm 0.02 m_{max}$ is the maximum value of τ_b/N (O. et al., 2007; Schoof, 2005). m_{max} is the maximum bedrock slope. A_s $(m\,Pa^{-n}yr^{-1})$ is the sliding parameter. The sliding parameter A_s is defined as (O. et al., 2007):

$$A_s = B\lambda + \frac{-2\times10^{-5} + 0.013r + 0.0262r^2}{r^2} \quad (5)$$

where $B = 430 \pm 40 MPa^{-3}yr^{-1}$ is the ice fluidity parameter under isothermal conditions (Louis and Lliboutry, 1987); λ is the bedrock obstacle wavelength; r is the bedrock roughness coefficient (Gudmundsson, 1997; Schoof, 2005; Berends et al., 2023), calculated via root mean square height (RMSH) (Shepard et al., 2001; Berti et al., 2013):

$$r = \sqrt{\frac{1}{k-1}\sum_{i=1}^{k}(z_i - \bar{z})^2} \quad (6)$$

where k is the moving windows size (number of cells), z_i is the cell elevation, and $\bar{z}$ is the mean elevation within the window (Berti et al., 2013).

2.3 Accuracy assessment

This study evaluates three ice thickness models (GV14, GV22, ITMSL) applied to 16 HMA glaciers. Model performance is quantified using five statistical metrics: root mean square error (RMSE), standard deviation (STD), mean error (ME), relative error (RE), and correlation coefficient (CC) (Höhle and Höhle, 2009; Liu et al., 2019; Chen et al., 2022; González-Moradas and Viveen, 2020; Pang et al., 2023). These metrics are defined as:

$$\mathrm{RMSE} = \sqrt{\frac{\sum_{i=1}^{n}(H_{GPR,i} - H_{mod,i})^2}{n}} \quad (7)$$

https://doi.org/10.5194/egusphere-2025-5838
Preprint. Discussion started: 26 January 2026
© Author(s) 2026. CC BY 4.0 License.

$$\mathrm{STD} = \sqrt{\frac{\sum_{i=1}^{n}(H_{GPR,i} - H_{mod,i} - \frac{1}{n}\sum_{i=1}^{n}(H_{GPR,i} - H_{mod,i}))^2}{n-1}} \quad (8)$$

$$\mathrm{ME} = \frac{1}{n}\sum_{i=1}^{n}(H_{GPR,i} - H_{mod,i}) \quad (9)$$

$$\mathrm{RE} = \frac{(H_{GPR,i} - H_{mod,i})}{H_{GPR,i}} \quad (10)$$

$$\mathrm{CC} = \frac{\sum_{i=1}^{n}((H_{GPR,i} - \frac{1}{n}\sum_{i=1}^{n} H_{GPR,i})(H_{mod} - \frac{1}{n}\sum_{i=1}^{n} H_{mod,i}))}{\sqrt{\sum_{i=1}^{n}(H_{GPR,i} - \frac{1}{n}\sum_{i=1}^{n} H_{GPR,i})^2}\sqrt{\sum_{i=1}^{n}(H_{mod,i} - \frac{1}{n}\sum_{i=1}^{n} H_{mod,i})^2}} \quad (11)$$

where $H_{GPR,i}$ is the ice thickness measured by GPR at point i, $H_{mod,i}$ is the modelled ice thickness at point i, and n is the total number of GPR points.

RMSE quantifies the overall magnitude of errors between modelled and GPR measured ice thickness, serving as a composite measure of accuracy. STD of residuals characterizes the dispersion of model errors around their mean value, reflecting simulation stability. ME indicates systematic bias, with positive or negative values denoting overestimation or underestimation. RE expresses the absolute percentage deviation of modelled ice thickness from observations. CC measures the strength of linear relationship between modelled and measured thickness, where values approaching 1 indicate strong positive agreement. Collectively, these complementary metrics provide a comprehensive assessment of model performance in terms of accuracy, precision, bias, and consistency with observed spatial patterns.

3 Model Instructions

Model performance was validated using in situ ice thickness measurements from 16 glaciers across HMA. The experiments were driven by glacier surface velocities, topographic data, and glacier inventory. An initial simulation was conducted based on a set of assumptions, followed by iterative refinement until the results met the predefined convergence criteria. The iterative procedure for estimating glacier thickness using the ITMSL model comprises the following steps (Figure 2.):

(1) Input Data: Provide the DEM, glacier surface velocity field, and glacier outlines.

(2) Preprocessing: Extract the glacier mask from the outlines. Calculate the glacier surface slope (α) from the DEM, respectively. Initial u_b to 0.

(3) Initial ice thickness: Use laminar flow theory (Equation 1) to compute the initial ice thickness (H_0).

(4) Shape Factor Calculation: Determine glacier width (w) as the mean distance from the centerline to the glacier margins. Calculate the valley shape factor （f） using Equation 3, incorporating w and H_0.

https://doi.org/10.5194/egusphere-2025-5838
Preprint. Discussion started: 26 January 2026
© Author(s) 2026. CC BY 4.0 License.

(5) Basal shear stress: Bring f, H_0, α, and ice density (ρ) into equation 2 to derive τ_b .

(6) Initial Bed Topography: Obtain the initial subglacial topography (Z_0) by subtracting H_0 from the surface DEM.

(7) Sliding Law Parameters: Calculate the ice bed slope from Z_0. Calculate the maximum slope ratio (C) and bedrock roughness (r) (Equation 6). Determine the sliding parameter (A_s) via Equation 5. Estimate effective pressure (N) using H_0 and Z_0.

(8) Basal Sliding Velocity: Put τ_b, N, C, A_s, and n into equation 4 for iterative calculation, thus obtaining u_b.

(9) Updated Ice Thickness: Substitute the newly-obtained u_b into Equation 1 to recompute ice thickness (H_i).

(10) Convergence Check: Calculate the difference in glacier mean thickness between iterations: $\Delta H = H_i - H_{i-1}$. If ΔH is less than the threshold, the final glacier thickness and subglacial topography are output. Else, H_i is updated to H_{i-1} and return to Step3.

https://doi.org/10.5194/egusphere-2025-5838
Preprint. Discussion started: 26 January 2026
© Author(s) 2026. CC BY 4.0 License.

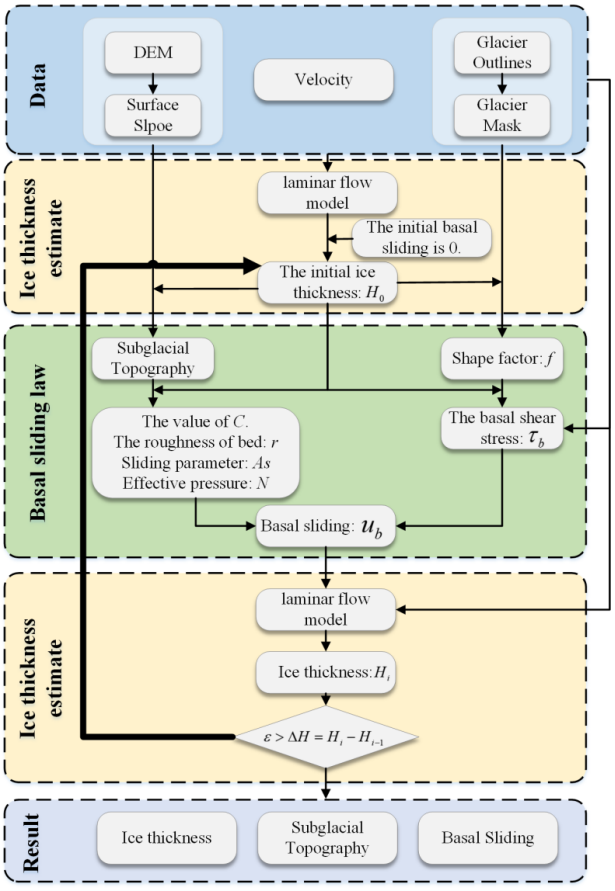

Figure 2: Flow chart of glacier thickness inversion using ITMSL model.

4 Model experiments

4.1 Calibration of ITMSL model

This study presents an ITMSL ice thickness model. To evaluate its performance, the model was applied to 16 HMA glaciers. The ice fluidity parameter B was calibrated against GPR ice thickness measurements, with a value range of $390 - 470\mathrm{MPa}^{-3}\mathrm{yr}^{-1}$ determined based on the existing studies (Louis and Lliboutry, 1987; Cuffey and Paterson, 2010). We systematically tested B values at $5\mathrm{MPa}^{-3}\mathrm{yr}^{-1}$ interval to quantify its influence on thickness estimates, while other parameters were either literature-derived or glacier-specific. The optimal B value for each glacier was determined by minimizing RMSE between

https://doi.org/10.5194/egusphere-2025-5838
Preprint. Discussion started: 26 January 2026
© Author(s) 2026. CC BY 4.0 License.

modeled and GPR measured thickness. These calibrated parameters provide reference values for regional ice thickness inversions in unmeasured HMA glacier (Table 2).

For the 16 selected glaciers, the calibrated optimal B values ranged $425 - 470\ \mathrm{MPa^{-3}yr^{-1}}$, with a regional optimum of $465\ \mathrm{MPa^{-3}yr^{-1}}$ (Figure 3). 13 glaciers exhibited B exceeding $460\ \mathrm{MPa^{-3}yr^{-1}}$, while QIYI, SIGH, and TSTU showed values below $460\ \mathrm{MPa^{-3}yr^{-1}}$. Several factors contribute to variations in parameter values, including model itself, accuracy of input data, and potential inconsistencies in the timing of input data acquisition compared to GPR measurements.

Table 2. The optimal fluidity parameters of each glacier calculated by GPR.

Glacier	B ($\mathrm{MPa^{-3}yr^{-1}}$)	Glacier	B ($\mathrm{MPa^{-3}yr^{-1}}$)
BARP	465	SARY	470
BATU	470	SHQI	465
CHHU	465	CTSG	465
GHAR	470	SHIY	470
HXLG	470	SIGH	455
HEIG	460	TSTU	435
PASU	470	URUM	470
QIYI	425	Total	465
SACH	465		

https://doi.org/10.5194/egusphere-2025-5838
Preprint. Discussion started: 26 January 2026
© Author(s) 2026. CC BY 4.0 License.

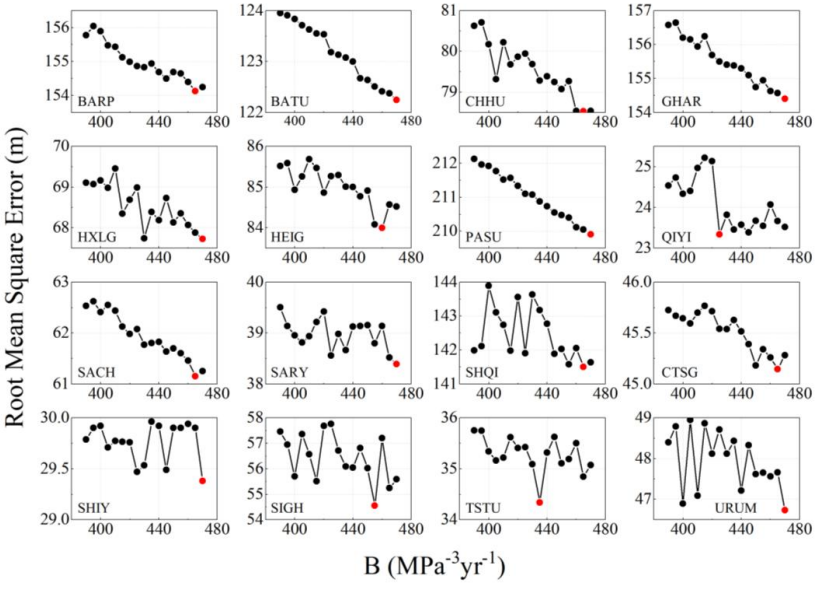

Figure 3: RMSE values of ice thickness inversion when the ITMSL model takes different B values.

4.2 Ice thickness distribution and subglacial topography

Using calibrated parameters, we applied the ITMSL model to estimate thickness distributions across the 16 study glaciers. For comparison, we also referred to the ice thickness estimates derived from the laminar flow theory-based GV14 and GV22 models (Gantayat et al., 2014; Millan et al., 2022). Figure 4 illustrates modeled thickness patterns for CTSG glacier under the three models. Figure 5 details CTSG's subglacial topography, surface velocity, basal sliding velocity, and the ratio of basal velocity to surface velocity. Parallel analyses performed on the remaining 15 glaciers yielded comprehensive ice thickness, bed topography, and basal sliding datasets (Table 4).

At CTSG glacier, GPR measurements across validation points indicated a mean ice thickness of 172.88 m. The ITMSL model produced a mean thickness of 114.63 m and a total glacier volume of 1.5277 km^3. Spatially, all three models (ITMSL, GV14, GV22) consistently captured characteristic thickness patterns: maximum along the central flowline and minimum in tributaries and marginal zones. Quantitatively, ITMSL (114.63 m), GV22 (104.90 m), and GV14 (98.39 m) showed divergent mean estimates, with GV14 producing systematically lower values. Crucially, ITMSL exhibited closest agreement with GPR data, indicating superior accuracy relative to the comparison models.

https://doi.org/10.5194/egusphere-2025-5838
Preprint. Discussion started: 26 January 2026
© Author(s) 2026. CC BY 4.0 License.

GPR surveys delineated 5 cross-sections (CS1-CS5) at CTSG glacier (Figure 4). We evaluated ice thickness accuracy at each CS using RMSE for three models (Table 3). ITMSL demonstrated superior performance at CS1, CS4, and CS5 with RMSE values of 34.4m, 47.4m, and 24.5m respectively, outperforming GV14 (40.5m, 65.6m, 33.6m) and GV22 (98.2m, 69.9m, 64.8m). Conversely, GV22 achieved lower RMSE at central flowline sections CS2 (29.4m) and CS3 (42.1m), compared to ITMSL (40.9m, 57.4m) and GV14 (51.7m, 70.4m).

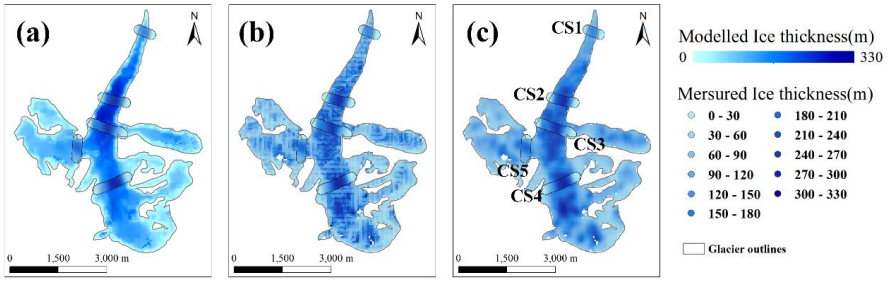

Figure 4: CTSG glacier thickness estimated by the three models. (a) GV22, (b) GV14, (c) ITMSL.

Table 3: Accuracy of ice thickness estimates for five cross-sections of the CTSG glacier.

	RMSE			STD			ME			RE			CC		
	ITMSL	GV14	GV22	ITMSL	GV14	GV22	ITMSL	GV14	GV22	ITMSL	GV14	GV22	ITMSL	GV14	GV22
CS1	34.38	40.50	98.20	15.65	27.24	11.32	32.20	32.22	97.55	0.21	0.23	0.69	0.91	0.63	0.74
CS2	40.95	51.69	29.35	40.93	46.56	29.15	1.08	22.46	-3.47	-0.24	-0.12	-0.10	0.95	0.77	0.90
CS3	57.37	70.45	42.14	49.28	69.18	37.75	-29.37	-13.31	-18.73	-0.70	-0.56	-0.45	0.87	0.48	0.89
CS4	47.41	65.56	69.92	43.89	65.49	61.22	-17.94	-2.97	33.79	-0.82	-0.94	-0.36	0.93	0.76	0.92
CS5	24.53	33.60	64.81	23.88	23.53	25.74	5.60	23.99	59.48	0.02	0.14	0.35	0.69	0.74	0.74
Total	45.25	58.06	57.77	44.48	57.62	54.30	-8.33	7.20	19.72	-0.42	-0.35	-0.12	0.82	0.66	0.73

Figure 5a reconstructs the subglacial topography of CTSG glacier by subtracting modelled ice thickness from the DEM-derived surface elevation. The accuracy of this reconstructed bed topography is contingent upon the precision of both the ice thickness estimates and the input DEM. Analysis of basal sliding velocity reveals a glacier-wide mean of 5.53 m/yr., This velocity exhibits a strong spatial correlation with surface velocity (R = 0.799), with a mean ratio of 0.399 (u_b/u_s). These findings demonstrate that basal sliding affects ice thickness distribution in laminar flow theory, necessitating explicit representation of sliding dynamics for accurate glacier simulations. The quantified u_b/u_s ratio

https://doi.org/10.5194/egusphere-2025-5838
Preprint. Discussion started: 26 January 2026
© Author(s) 2026. CC BY 4.0 License.

further provides critical constraints on glacial dynamical behavior, underscoring its essential role in advancing ice thickness inversion methodologies.

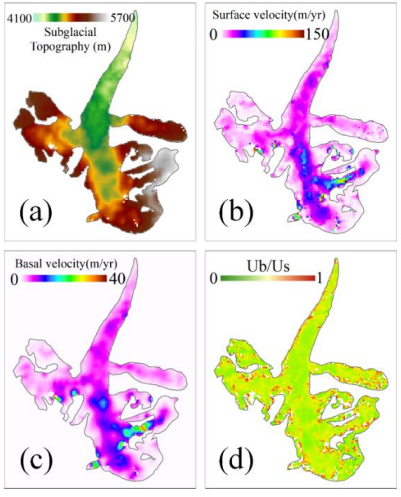

Figure 5: (a) CTSG glacier subglacial topography, (b) surface velocity, (c) basal sliding, and (d) the ratio of sliding velocity to surface velocity.

We applied the ITMSL model to estimate ice thickness and basal sliding velocity across the selected glaciers (Table 4). Modeled ice thickness values represents point-specific averages collocated with GPR measurements. Results indicate systematic overestimation for 12 glaciers and underestimation for four. This bias suggests inherent limitations in laminar flow parameterization, particularly regarding basal sliding. The derived u_b/u_s ratio ranges from 0.342 to 0.457—significantly exceeding GV14's assumed 0.25, which induces substantial thickness overestimation. Consequently, incorporating the physically-based sliding law enhances laminar flow theory by explicitly representing subglacial processes, thereby improving region ice thickness estimation accuracy.

Table 4: Ice thickness and movement characteristics of 16 glaciers.

Glacier	GPR (m)	GV14 (m)	GV22 (m)	ITMSL (m)	u_s (m/yr)	u_b (m/yr)	u_b/u_s
BARP	120.95	143.86	191.74	163.90	125.70	42.35	0.350
BATU	127.06	142.37	211.63	157.94	101.34	36.35	0.342
CHHU	103.93	113.63	142.55	127.08	108.40	44.92	0.391
GHAR	152.94	114.62	153.15	138.11	81.06	31.08	0.366
HXLG	43.96	83.91	42.60	83.47	10.70	4.25	0.457

https://doi.org/10.5194/egusphere-2025-5838
Preprint. Discussion started: 26 January 2026
© Author(s) 2026. CC BY 4.0 License.

HEIG	114.87	94.88	68.75	106.43	24.97	9.65	0.385
PASU	145.55	156.36	185.24	163.58	162.08	59.89	0.368
QIYI	77.81	63.58	53.26	59.14	8.65	3.34	0.401
SACH	121.79	123.40	185.03	131.01	40.90	16.56	0.388
SARY	75.52	77.80	81.28	77.68	8.82	3.32	0.415
SHQI	38.68	71.31	80.88	71.16	21.63	7.92	0.354
CTSG	172.88	104.90	98.39	114.63	15.48	5.53	0.399
SHIY	39.47	49.18	30.09	52.83	7.78	2.95	0.398
SIGH	68.93	71.99	42.28	72.0	7.01	2.63	0.399
TSTU	51.63	64.63	63.55	60.21	4.61	1.78	0.422
URUM	40.05	78.45	45.61	83.85	20.51	7.67	0.415

4.3 Accuracy assessment of the glacier thickness

Comprehensive evaluation of the ITMSL model against GV14, GV22 using 5 statistical metrics applied to GPR-validated thickness data (Figure 6) demonstrates significant improvements: ITMSL achieves higher correlation coefficients than GV22 in 8 of 16 glaciers and surpasses GV14 in 12 of 16, indicating stronger linear relationships with observations; reduces STD to 41.31m (28.87% lower than GV22's 58.08m and 16.17% below GV14's 49.28m), with particularly notable decreases at BATU (down 60.5%) and HXLG (down 37.9%); and achieves 17% lower RMSE (56.72m) than GV22 (68.34m) and 12.6% reduction versus GV14 (64.92 m). Although 4 glaciers (SHIY, HXLG, URUM, HEIG) exhibit higher deviation than GV22—likely due to complex subglacial topography—and mean/relative errors show limited changes, the consistent precision enhancements confirm ITMSL's superior reliability across most glaciers. These advances stem directly from the physically constrained basal sliding parameterization, which effectively mitigates GV14's problematic u_b/u_s assumption of 0.25 that systematically overestimates thickness. ITMSL thus represents a significant advancement for ice thickness estimation, while also highlighting the limitations of the ITMSL model requiring further refinement.

Despite inherent limitations in input data quality and model parameterization, the ITMSL model demonstrates robust performance across diverse HMA glaciers (Figure 6), though localized discrepancies persist in topographically complex regions. Inter-model variations primarily arise from uncertainties in

https://doi.org/10.5194/egusphere-2025-5838
Preprint. Discussion started: 26 January 2026
© Author(s) 2026. CC BY 4.0 License.

foundational datasets, particularly DEM precision, surface velocity accuracy, and slope derivation errors. Crucially, the convergence of ITMSL with established models (GV14 and GV22) validates its utility as a physically constrained framework for regional glacier thickness distribution mapping. Estimation accuracy can be further enhanced through integration of multi-temporal velocity products, optimization of sliding law parameters, and assimilation of subglacial topography constraints.

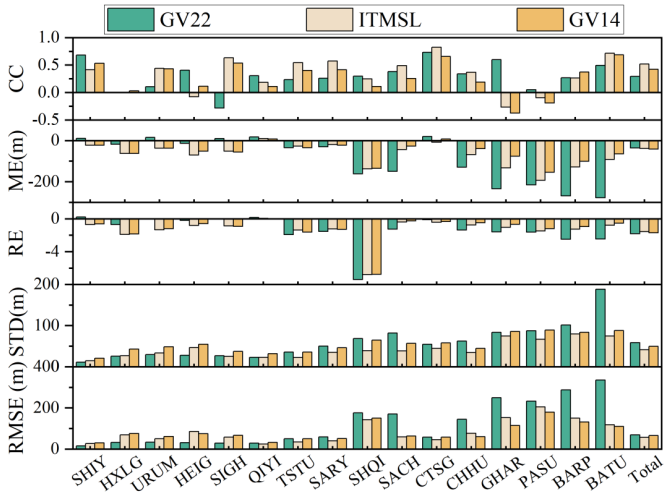

Figure 6: Accuracy of glacier thickness estimated by three ice thickness models based on laminar flow theory.

5 Discussion

5.1 Analysis of factors affecting the accuracy of simulated ice thickness

Using glacier-specific characteristics, we iteratively computed key parameters, including the valley shape factor (f), effective stress (N), basal sliding velocity (u_b), sliding parameter (A_s), and bedrock roughness (r), to derive ice thickness distributions across the 16 glaciers. Although ITMSL demonstrated improvements, locailzed accuracy deficits at 4 glaciers (SHIY, HXLG, URUM, HEIG) necessitate targeted analysis. Ice thickness model accuracy is governed by 4 factors: 1) input data quality (DEM, surface velocity, glacier outline); 2) model limitations; 3) parameterization uncertainties; and 4) glacier characteristics (slope, aspect, bedrock topography) (Frey et al., 2014; Pang et al., 2023; Wang et al., 2023). For URUM glacier, analyzed as an integrated system incorporating both eastern and western branches (Wang et al., 2016), we quantified performance using STD.

https://doi.org/10.5194/egusphere-2025-5838
Preprint. Discussion started: 26 January 2026
© Author(s) 2026. CC BY 4.0 License.

Statistical analysis of glacier geometry and dynamics (Figure 7) revealed distinct characteristics for 4 glaciers that showed limited improvement in accuracy: SHIY (length: 926m, area: 0.495km^2, width: 534m), HXLG (length: 1499m, area: 1.099km^2, width: 733m), and the eastern branches (URUME; length: 2012m, area: 1.03km^2, width: 513m) and western branches (URUMW; length: 1694m, area: 0.55km^2, width: 322m) of the URUM glacier. While sharing comparable elevation, velocity, and slope characteristics with other glaciers, their constrained dimensions, particularly sub 1km^2 areas and sub 750m widths, exacerbate 4 four key limitations: First, reduced glacier dimensions challenges ice thickness inversion due to insufficient grid representation. Second, spatial resolution mismatches between modelled ice thickness (50m cells) and GPR point spacing (1.5-5m) amplify errors. Third, data gaps in remote sensing, derived velocity fields propagate through thickness calculations. Finally, inherent model uncertainties in ice density parameterization, sliding coefficient calibration, and bedrock roughness estimation contribute to inaccuracies. Addressing these multiscale challenges—spanning data acquisition, model structure, and parameter sensitivity—remains essential for enhancing ITMSL's reliability across diverse glacial regimes.

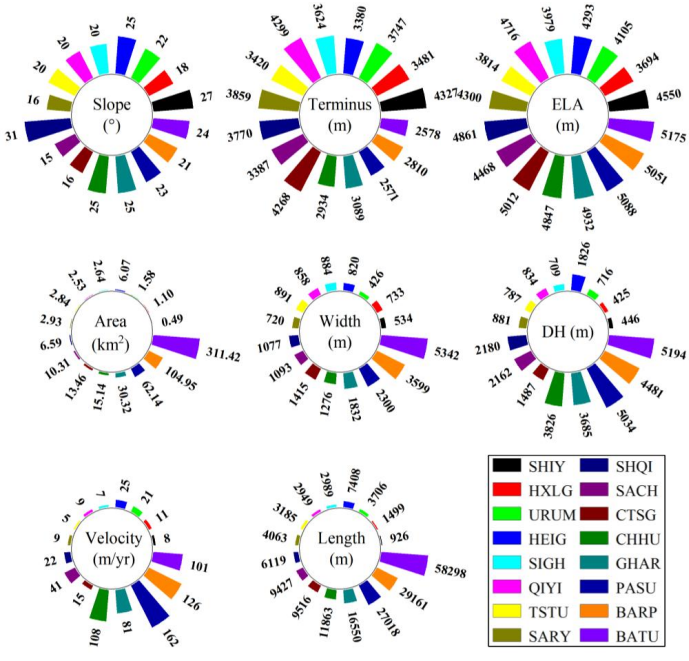

Figure 7: Geometric and dynamic characteristics of selected glaciers, showing length derived from centerline, width calculated as area to length ratio, and equilibrium line altitude represented by median elevation.

https://doi.org/10.5194/egusphere-2025-5838
Preprint. Discussion started: 26 January 2026
© Author(s) 2026. CC BY 4.0 License.

5.2 Influence of glacier basal sliding on the ice thickness

Building upon established glaciological (Schoof, 2005; Gantayat et al., 2014; Zoet and Iverson, 2020; Millan et al., 2022), this study develops the ITMSL model by integrating basal sliding law into laminar flow theory. Comparative analysis at GPR measurement points (Figure 8) reveals distinct performance regimes tied to u_b/u_s: For u_b/u_s ranging from 0.1 to 0.4, ice thickness deviations follow GV14 > ITMSL > GV22, whereas in the 0.4-1.0 range ITMSL reduces absolute deviation relative to GV14 and GV22, respectively. Crucially, all models exhibit peak biases within the 0.2-0.5 u_b/u_s, where ITMSL achieves 57.4% and 46.9% lower deviations than GV14 and GV22, demonstrating how basal drag constraints fundamentally improve thickness estimation.

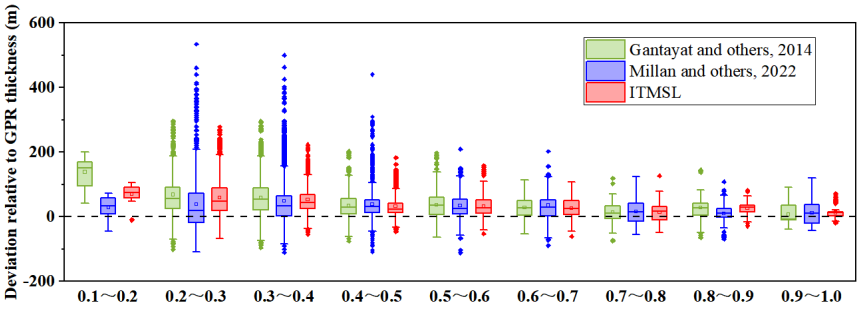

Figure 8: Comparative analysis of ice thickness estimation deviations for different ratios of basal sliding to surface velocity.

Beyond model intercomparison, we analyze the effects of basal sliding velocity on ice thickness estimation (Figure 9). The correlation coefficients between ice thickness bias and u_b are 0.2417 for GV14, 0.2802 for GV22, and 0.4711 for ITMSL, indicating ITMSL's heightened sensitivity to basal sliding. This enhanced physical responsiveness validates the efficacy of integrating basal drag constraints into laminar flow theory. Consequently, this integration significantly improves the robustness of thickness estimation across diverse glacial conditions.

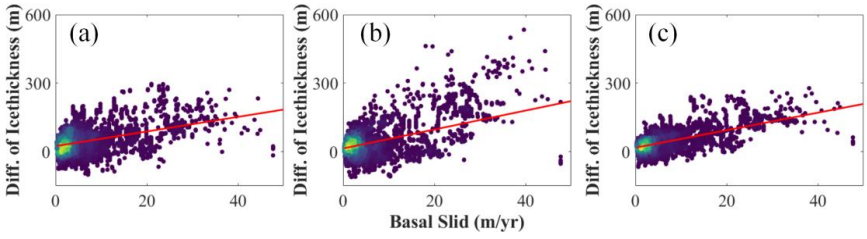

https://doi.org/10.5194/egusphere-2025-5838
Preprint. Discussion started: 26 January 2026
© Author(s) 2026. CC BY 4.0 License.

Figure 9: Deviations of ice thickness estimates from three laminar flow models at different basal sliding. (a) GV14; (b) GV22; (c) ITMSL.

5.3 Influence of DEMs on the ice thickness

Contemporary DEMs derive primarily from microwave (InSAR) and optical (stereophotogrammetry) sensors (González-Moradas and Viveen, 2020; Chen et al., 2022; Hawker et al., 2022), typically referenced to EGM2008 geoid or WGS84 ellipsoid vertical datums (González-Moradas and Viveen, 2020; Chymyrov, 2021). These open access DEMs (2000-2019 acquisition) exhibit significant temporal spatial inconsistencies affecting ice thickness inversion (Fan et al., 2022), with spatial resolutions ranging from 30 to 90m (González-Moradas and Viveen, 2020; Chymyrov, 2021).

We evaluated five 30m resolution DEMs—GLOB30 (TanDEM-X, 2010-2015), ASTER v3 (optical, 2019), AW3D (optical, 2006-2011), NASADEM (SRTM, 2000), and TanDEM-30 (2010-2015)—for ice thickness estimation across 16 HMA glaciers using GPR measurements (Figure 10) (Frey and Paul, 2012; Abrams et al., 2020; González-Moradas and Viveen, 2020; Fan et al., 2022; Hawker et al., 2022). Results show that GLOB-30 (STD 41.31m) and TanDEM-30 (41.20m) outperformed ASTER (46.37m), AW3D (42.09m), and NASADEM (47.63m). GLOB30/TanDEM-30 achieved highest accuracy for 9 of the 16 glaciers, which is different from the 90m-resolution NASADEM preferred by Chen et al. (2022). 30m DEMs reduce slope smoothing artifacts, which explains its higher accuracy than the 90m products. This analysis establishes high-resolution DEMs (GLOB30/TanDEM-30) as optimal for HMA glacier thickness inversion, resolving terrain complexities inadequately captured by optical/SRTM-derived products.

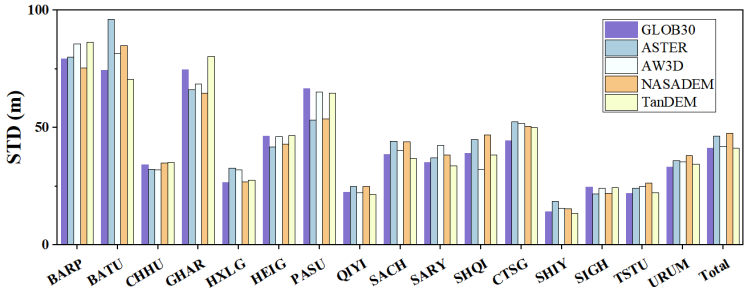

Figure 10: To estimate the standard deviation (STD) of ice thicknesses for the 16 glaciers, we used GLOB30, ASTER, AW3D, NASADEM, and TanDEM-30 as input DEMs.

https://doi.org/10.5194/egusphere-2025-5838
Preprint. Discussion started: 26 January 2026
© Author(s) 2026. CC BY 4.0 License.

5.4 Comparison with existing ice thicknesses

To contextualize ITMSL, GV14, and GV22 within broader glaciological modelling, we compared their thickness estimates with 4 established models (Composite, GlabTop2, H-F, and OGGM) using GPR measured ice thickness across 16 HMA glaciers (Figure 11) (Huss and Farinotti, 2012; Frey et al., 2014; Farinotti et al., 2019; Maussion et al., 2019). Model data were sourced from Farinotti et al. (2019), with methodological foundations including mass conservation approaches (OGGM, H-F); shallow ice approximation theory (GlabTop2), and weighted multi-model ensembles (Composite). Systematic analysis reveals consistent ice thickness overestimation across all seven models for at least 8 of the 16 glaciers, with laminar flow-based models (ITMSL, GV14, GV22) exhibiting particularly pronounced deviations—exceeding other models' estimates for 9 glaciers. GV22 uniquely overestimated SACH, CHHU, GHAR, BARP, and BATU glaciers, while ITMSL and GV14 dominated overestimation at SHIY, HXLG, and URUM. Comparison with the GPR ice thickness (61.24 m) shows that the thickness is estimated to be 100.65 m (64.4%) for ITMSL, 104.05 m (69.9%) for GV14, 97.46 m (59.1%) for GV22, while it is 84.91 m (38.7%) for Composite, 81.32 m (32.8%) for GlabTOP2, 80.13 m (30.8%) for H-F, and 75.55 m (23.4%) for OGGM. This suggests that current ice thickness models have been overestimating glacier thickness.

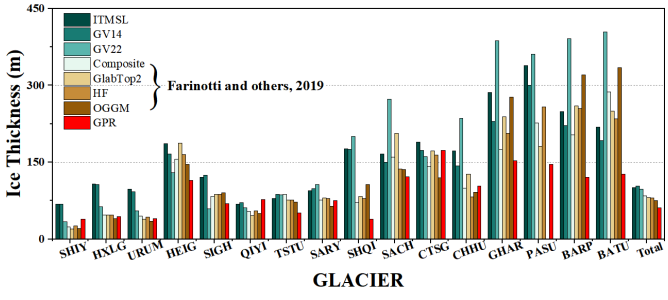

Figure 11: Comparative analysis of the ice thickness of 16 glaciers estimated by 7 models (ITMSL, GV14, GV22, Composite, GlabTop2, H-F, and OGGM) and GPR measurements.

Comprehensive accuracy assessment reveals consistent ice thickness overestimation across all models, though ITMSL effectively constrains GV22's excessive deviations as evidenced by thickness distributions (Figure 12). ME quantification confirms systematic positive bias, with the Composite demonstrating relative improvements—reducing thickness error by 13.1% versus OGGM, 13.2% against GlabTop2, 2.4% compared to H-F, 39.1% relative to GV22, 28.2% below GV14, and 14.3% less than

https://doi.org/10.5194/egusphere-2025-5838
Preprint. Discussion started: 26 January 2026
© Author(s) 2026. CC BY 4.0 License.

ITMSL. These findings validate multi-model ensemble approaches for leveraging complementary strengths through error compensation mechanisms, though absolute accuracy requires further enhancement given persistent overestimation trends.

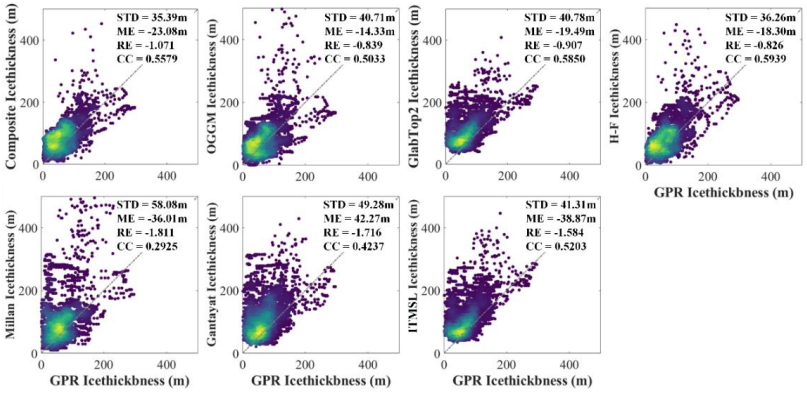

Figure 12: The accuracy of ice thickness estimates from 7 models for 16 glaciers was evaluated and compared with ice thickness measured by GPR.

Subglacial topography was reconstructed by subtracting modelled ice thickness from GLOB30 surface elevations, with validation against GPR-derived bed measurements (Figure 13). The modeled and observed ice beds show excellent agreement, with correlation coefficients exceeding 0.97 across all seven models and relative errors below 0.4%. The high-fidelity reproduction of basal geometry—achieved despite complex subglacial terrain—confirms the robustness of inversion methodologies for applications requiring precise bed mapping, particularly potential glacial lake research.

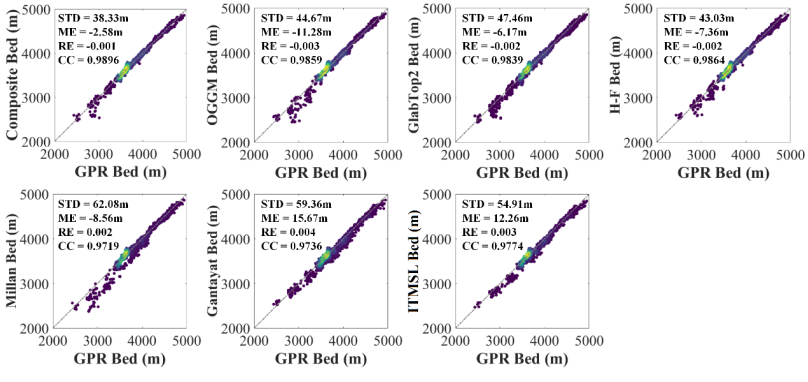

Figure 13: The accuracy of ice bed estimates from 7 models for 16 glaciers was evaluated and compared with the ice bed measured by GPR.

https://doi.org/10.5194/egusphere-2025-5838
Preprint. Discussion started: 26 January 2026
© Author(s) 2026. CC BY 4.0 License.

6 Conclusions and perspectives

This study presents a novel glacier thickness inversion model, ITMSL, which enhances traditional laminar flow theory by incorporating a physically-based basal sliding law. Applied to 16 glaciers across High Mountain Asia (HMA), ITMSL model autonomously estimates basal sliding velocity, ice thickness distribution, and subglacial topography with significantly improved accuracy—reducing STD by 16.2% compared to GV14 and 28.9% versus GV22. This study highlighted the importance of considering glacier basal sliding in ice thickness estimates, particularly when u_b/u_s is greater than 0.4. While ITMSL demonstrates robust performance for glaciers area larger than 1 km², its efficacy diminishes for narrower glaciers. Additionally, the evaluation of 5 DEMs showed that TanDEM-30 and GLOB30 as optimal inputs for ice thickness estimation in HMA, which provides valuable guidance for the selection of DEMs in future studies.

With the growing availability of high-resolution remote sensing data, ITMSL shows great potential for glacier thickness estimation. However, the ITMSL does not account for the effects of glacier temperature and surface debris on ice thickness estimation, and lacked verification of modeled glacier sliding measurements. Despite these limitations, ITMSL model establishes a promising foundation for estimating ice thickness in complex mountain environments, particularly where traditional laminar flow assumptions prove inadequate.

Code and data availability

The current version of ITMSL is available from the project website https://github.com/pxgxhcxhs/ITMSL (last access: 24 November 2025) under the GNU General Public License (GPL) v3.0. The exact version of the model used to produce the results used in this paper is archived on Zenodo under https://doi.org/10.5281/zenodo. 18267363 (Pang et al., 2025), as are input data and scripts to run the model and produce the plots for all the simulations presented in this paper (Pang et al., 2025).

https://doi.org/10.5194/egusphere-2025-5838
Preprint. Discussion started: 26 January 2026
© Author(s) 2026. CC BY 4.0 License.

Author contribution

XP is the main ITMSL developer and wrote most of the paper. LJ conceived and designed the research. YW tested the model and assisted with design and debugging. XL carried out the model validation and accuracy assessment with contributions from YL and XL. TY revised the article.

Competing interests

The contact author has declared that none of the authors has any competing interests.

Acknowledgments

We acknowledge the open-access glacier inventory and GlaThiDa dataset from the National Snow and Ice Data Center (NSIDC), the Copernicus DEM from ESA, and the glacier velocity data from Millan et al (2022). This research was funded by the National Natural Science Foundation of China (Grant No. 42174046), the Second Qinghai-Tibet Plateau Scientific Expedition and Research Program, No.2019QZKK0905.

References

Abrams, M., Crippen, R., and Fujisada, H.: ASTER Global Digital Elevation Model (GDEM) and ASTER Global Water Body Dataset (ASTWBD), Remote Sensing, 12, 10.3390/rs12071156, 2020.

Azam, M. F., Wagnon, P., Ramanathan, A., Vincent, C., Sharma, P., Arnaud, Y., Linda, A., Pottakkal, J. G., Chevallier, P., and Singh, V. B.: From balance to imbalance: a shift in the dynamic behaviour of Chhota Shigri glacier, western Himalaya, India, Journal of Glaciology, 58, 315-324, doi:10.3189/2012JoG11J123, 2012.

Bahr, D. B., Pfeffer, W. T., and Kaser, G.: A review of volume-area scaling of glaciers, Rev. Geophys., 53, 95-140, 10.1002/2014rg000470, 2015.

Becek, K., Koppe, W., and Kutoğlu, Ş.: Evaluation of Vertical Accuracy of the WorldDEM™ Using the Runway Method, Remote Sensing, 8, 10.3390/rs8110934, 2016.

Berends, C. J., van de Wal, R. S. W., van den Akker, T., and Lipscomb, W. H.: Compensating errors in inversions for subglacial bed roughness: same steady state, different dynamic response, The Cryosphere, 17, 1585-1600, 10.5194/tc-17-1585-2023, 2023.

Berti, M., Corsini, A., and Daehne, A.: Comparative analysis of surface roughness algorithms for the identification of active landslides, Geomorphology, 182, 1-18, 10.1016/j.geomorph.2012.10.022, 2013.

Bolch, T., Kulkarni, A., Kaab, A., Huggel, C., Paul, F., Cogley, J. G., Frey, H., Kargel, J. S., Fujita, K., Scheel, M., Bajracharya, S., and Stoffel, M.: The state and fate of Himalayan glaciers, Science, https://doi.org/10.1093/9780197802601.003.0002, 2012.

https://doi.org/10.5194/egusphere-2025-5838
Preprint. Discussion started: 26 January 2026
© Author(s) 2026. CC BY 4.0 License.

Brun, F., Berthier, E., Wagnon, P., Kaab, A., and Treichler, D.: A spatially resolved estimate of High Mountain Asia glacier mass balances from 2000 to 2016, Nature Geoscience, 10, 668-+, 10.1038/ngeo2999, 2017.

Budd, W. F., Keage, P. L., and Blundy, N. A.: Empirical studies of ice sliding, Journal of Glaciology, 23, 157-170, doi:10.3189/S0022143000029804, 1979.

Chen, W. F., Yao, T. D., Zhang, G. Q., Li, F., Zheng, G. X., Zhou, Y. S., and Xu, F. L.: Towards ice-thickness inversion: an evaluation of global digital elevation models (DEMs) in the glacierized Tibetan Plateau, Cryosphere, 16, 197-218, 10.5194/tc-16-197-2022, 2022.

Chymyrov, A.: Comparison of different DEMs for hydrological studies in the mountainous areas, The Egyptian Journal of Remote Sensing and Space Science, 24, 587-594, 10.1016/j.ejrs.2021.08.001, 2021.

Cuffey, K. and Paterson, W.: The Physics of Glaciers Fourth Edition, 2010.

Echelmeyer, K. and Zhongxiang, W.: Direct Observation of Basal Sliding and Deformation of Basal Drift at Sub-Freezing Temperatures, Journal of Glaciology, 33, 83-98, 10.3189/S0022143000005396, 1987.

Engelhardt, H. and Kamb, B.: Basal sliding of Ice Stream B, West Antarctica, Journal of Glaciology, 44, 223-230, https://doi:10.3189/S0022143000002562, 1998.

Fan, Y., Ke, C.-Q., Zhou, X., Shen, X., Yu, X., and Lhakpa, D.: Glacier mass-balance estimates over High Mountain Asia from 2000 to 2021 based on ICESat-2 and NASADEM, Journal of Glaciology, 1-13, 10.1017/jog.2022.78, 2022.

Fang, K., Mei, Z., Wu, H., Zhou, F., Seppä, H., and Guo, Z.: Indian summer monsoon drives synchronous interdecadal hydroclimate changes in the Tibetan Plateau and surroundings, Global and Planetary Change, 234, 10.1016/j.gloplacha.2024.104379, 2024.

Farinotti, D., Huss, M., Fürst, J. J., Landmann, J., Machguth, H., Maussion, F., and Pandit, A.: A consensus estimate for the ice thickness distribution of all glaciers on Earth, Nature Geoscience, 12, 168-173, 10.1038/s41561-019-0300-3, 2019.

Farinotti, D., Brinkerhoff, D. J., Furst, J. J., Gantayat, P., Gillet-Chaulet, F., Huss, M., Leclercq, P. W., Maurer, H., Morlighem, M., Pandit, A., Rabatel, A., Ramsankaran, R., Reerink, T. J., Robo, E., Rouges, E., Tamre, E., van Pelt, W. J. J., Werder, M. A., Azam, M. F., Li, H. L., and Andreassen, L. M.: Results from the Ice Thickness Models Intercomparison eXperiment Phase 2 (ITMIX2), Frontiers in Earth Science, 8, 21, 10.3389/feart.2020.571923, 2021.

Farinotti, D., Brinkerhoff, D. J., Clarke, G. K. C., Fürst, J. J., Frey, H., Gantayat, P., Gillet-Chaulet, F., Girard, C., Huss, M., Leclercq, P. W., Linsbauer, A., Machguth, H., Martin, C., Maussion, F., Morlighem, M., Mosbeux, C., Pandit, A., Portmann, A., Rabatel, A., Ramsankaran, R., Reerink, T. J., Sanchez, O., Stentoft, P. A., Singh Kumari, S., van Pelt, W. J. J., Anderson, B., Benham, T., Binder, D., Dowdeswell, J. A., Fischer, A., Helfricht, K., Kutuzov, S., Lavrentiev, I., McNabb, R., Gudmundsson, G. H., Li, H., and Andreassen, L. M.: How accurate are estimates of glacier ice thickness? Results from ITMIX, the Ice Thickness Models Intercomparison eXperiment, The Cryosphere, 11, 949-970, 10.5194/tc-11-949-2017, 2017.

Fowler, A. C. and Frank, F. C.: A theoretical treatment of the sliding of glaciers in the absense of cavitation, Philosophical Transactions of the Royal Society of London. Series A, Mathematical and Physical Sciences, 298, 637-681, doi:10.1098/rsta.1981.0003, 1981.

https://doi.org/10.5194/egusphere-2025-5838
Preprint. Discussion started: 26 January 2026
© Author(s) 2026. CC BY 4.0 License.

Frey, H. and Paul, F.: On the suitability of the SRTM DEM and ASTER GDEM for the compilation of topographic parameters in glacier inventories, International Journal of Applied Earth Observations & Geoinformation, 18, 480-490, https://doi.org/10.1016/j.jag.2011.09.020, 2012.

Frey, H., Machguth, H., Huss, M., Huggel, C., Bajracharya, S., Bolch, T., Kulkarni, A., Linsbauer, A., Salzmann, N., and Stoffel, M.: Estimating the volume of glaciers in the Himalayan–Karakoram region using different methods, The Cryosphere, 8, 2313-2333, 10.5194/tc-8-2313-2014, 2014.

Gantayat, P., Kulkarni, A. V., and Srinivasan, J.: Estimation of ice thickness using surface velocities and slope: case study at Gangotri Glacier, India, Journal of Glaciology, 60, 277-282, 10.3189/2014JoG13J078, 2014.

Gilbert, A., Gimbert, F., Gagliardini, O., and Vincent, C.: Inferring the Basal Friction Law From Long Term Changes of Glacier Length, Thickness and Velocity on an Alpine Glacier, Geophysical Research Letters, 50, 10.1029/2023gl104503, 2023.

González-Moradas, M. d. R. and Viveen, W.: Evaluation of ASTER GDEM2, SRTMv3.0, ALOS AW3D30 and TanDEM-X DEMs for the Peruvian Andes against highly accurate GNSS ground control points and geomorphological-hydrological metrics, Remote Sensing of Environment, 237, 111509, https://doi.org/10.1016/j.rse.2019.111509, 2020.

Grinsted, A.: An estimate of global glacier volume, The Cryosphere, 7, 141-151, 10.5194/tc-7-141-2013, 2013.

Gudmundsson, G. H.: Basal-flow characteristics of a non-linear flow sliding frictionless over strongly undulating bedrock, Journal of Glaciology, 43, 80-89, 10.3189/S0022143000002835, 1997.

Hawker, L., Uhe, P., Paulo, L., Sosa, J., Savage, J., Sampson, C., and Neal, J.: A 30 m global map of elevation with forests and buildings removed, Environmental Research Letters, 17, 10.1088/1748-9326/ac4d4f, 2022.

Helanow, C., Iverson, N. R., Woodard, J. B., and Zoet, L. K.: A slip law for hard-bedded glaciers derived from observed bed topography, Science Advances, 7, eabe7798, doi:10.1126/sciadv.abe7798, 2021.

Höhle, J. and Höhle, M.: Accuracy assessment of digital elevation models by means of robust statistical methods, ISPRS Journal of Photogrammetry and Remote Sensing, 64, 398-406, 10.1016/j.isprsjprs.2009.02.003, 2009.

Hugonnet, R., McNabb, R., Berthier, E., Menounos, B., Nuth, C., Girod, L., Farinotti, D., Huss, M., Dussaillant, I., Brun, F., and Kaab, A.: Accelerated global glacier mass loss in the early twenty-first century, Nature, 592, 726-731, 10.1038/s41586-021-03436-z, 2021.

Huss, M. and Farinotti, D.: Distributed ice thickness and volume of all glaciers around the globe, Journal of Geophysical Research: Earth Surface, 117, n/a-n/a, 10.1029/2012jf002523, 2012.

Iken, A.: The Effect of the Subglacial Water Pressure on the Sliding Velocity of a Glacier in an Idealized Numerical Model, Journal of Glaciology, 27, 407-421, doi:10.3189/S0022143000011448, 1981.

Joughin, I., Smith, B. E., and Schoof, C. G.: Regularized Coulomb Friction Laws for Ice Sheet Sliding: Application to Pine Island Glacier, Antarctica, GEOPHYSICAL RESEARCH LETTERS, 46, 4764-4771, 10.1029/2019GL082526, 2019.

Kraaijenbrink, P. D. A., Bierkens, M. F. P., Lutz, A. F., and Immerzeel, W. W.: Impact of a global temperature rise of 1.5 degrees Celsius on Asia's glaciers, Nature, 549, 257-260, 10.1038/nature23878, 2017.

Lannutti, E., Lenzano, M. G., Vacaflor, P., Rivera, A., Moragues, S., Gentile, M., and Lenzano, L.: Ice thickness distribution and stability of three large freshwater calving glaciers on the eastern side of

https://doi.org/10.5194/egusphere-2025-5838
Preprint. Discussion started: 26 January 2026
© Author(s) 2026. CC BY 4.0 License.

the Southern Patagonian Icefield, Cold Reg. Sci. Tech., 221, 10.1016/j.coldregions.2024.104158, 2024.

Li, F., Maussion, F., Wu, G., Chen, W., Yu, Z., Li, Y., and Liu, G.: Influence of glacier inventories on ice thickness estimates and future glacier change projections in the Tian Shan range, Central Asia, Journal of Glaciology, 1-15, 10.1017/jog.2022.60, 2022.

Li, H. L., Ng, F., Li, Z. Q., Qin, D. H., and Cheng, G. D.: An extended "perfect-plasticity" method for estimating ice thickness along the flow line of mountain glaciers, Journal of Geophysical Research Earth Surface, 117, -, https://doi.org/10.1029/2011JF002104, 2012.

Liang, P.-B. and Tian, L.-D.: Estimation of glacier ice storage in western China constrained by field ground-penetrating Radar surveys, Advances in Climate Change Research, https://doi.org/10.1016/j.accre.2022.04.002, 2022.

Liu, K., Song, C., Ke, L., Jiang, L., and Ma, R.: Global open-access DEM performances in Earth's most rugged region High Mountain Asia: A multi-level assessment, Geomorphology, 338, https://doi.org/10.1016/j.geomorph.2019.04.012, 2019.

Louis and Lliboutry: Realistic, yet simple bottom boundary conditions for glaciers and ice sheets, Journal of Geophysical Research, https://doi.org/10.1029/JB092iB09p09101, 1987.

Maussion, F., Butenko, A., Champollion, N., Dusch, M., Eis, J., Fourteau, K., Gregor, P., Jarosch, A. H., Landmann, J., Oesterle, F., Recinos, B., Rothenpieler, T., Vlug, A., Wild, C. T., and Marzeion, B.: The Open Global Glacier Model (OGGM) v1.1, Geoscientific Model Development, 12, 909-931, 10.5194/gmd-12-909-2019, 2019.

Miles, E., McCarthy, M., Dehecq, A., Kneib, M., Fugger, S., and Pellicciotti, F.: Health and sustainability of glaciers in High Mountain Asia, Nat. Commun., 12, 10, 10.1038/s41467-021-23073-4, 2021.

Millan, R., Mouginot, J., Rabatel, A., and Morlighem, M.: Ice velocity and thickness of the world's glaciers, Nature Geoscience, 15, 124-129, 10.1038/s41561-021-00885-z, 2022.

Millan, R., Mouginot, J., Rabatel, A., Jeong, S., Cusicanqui, D., Derkacheva, A., and Chekki, M.: Mapping Surface Flow Velocity of Glaciers at Regional Scale Using a Multiple Sensors Approach, Remote Sensing, 11, 10.3390/rs11212498, 2019.

O., Gagliardini, D., Cohen, P., Råback, and, T., and Zwinger: Finite-element modeling of subglacial cavities and related friction law, Journal of Geophysical Research Earth Surface, https://doi.org/10.1029/2006JF000576, 2007.

Pang, X., Jiang, L., Guo, R., Xu, Z., Li, X., and Lu, X.: Surface Motion and Topographic Effects on Ice Thickness Inversion for High Mountain Asia Glaciers: A Comparison Study from Three Numerical Models, Remote Sensing, 15, 10.3390/rs15225378, 2023.

Pang, X., Jiang, L., Wu, Y., Lu, X., Liu, Y., Li, X., and Yao, T.: ITMSL: an improved ice thickness inversion model integrating basal sliding dynamics for High Mountain Asia (v1.0.0), Zenodo, https://doi.org/10.5281/zenodo.18267363, 2025.

Pfeffer, W. T., Arendt, A. A., Bliss, A., Bolch, T., Cogley, J. G., Gardner, A. S., Hagen, J.-O., Hock, R., Kaser, G., Kienholz, C., Miles, E. S., Moholdt, G., Mölg, N., Paul, F., Radić, V., Rastner, P., Raup, B. H., Rich, J., and Sharp, M. J.: The Randolph Glacier Inventory: a globally complete inventory of glaciers, Journal of Glaciology, 60, 537-552, 10.3189/2014JoG13J176, 2014.

Radić, V. and Hock, R.: Regional and global volumes of glaciers derived from statistical upscaling of glacier inventory data, Journal of Geophysical Research, 115, 10.1029/2009jf001373, 2010.

https://doi.org/10.5194/egusphere-2025-5838
Preprint. Discussion started: 26 January 2026
© Author(s) 2026. CC BY 4.0 License.

Ramsankaran, R., Pandit, A., and Azam, M. F.: Spatially distributed ice-thickness modelling for Chhota Shigri Glacier in western Himalayas, India, Int. J. Remote Sens., 39, 3320-3343, 10.1080/01431161.2018.1441563, 2018.

Robel, A. A., Ultee, L., Ranganathan, M., and Nash, M.: For whom and by whom is glaciology?, Journal of Glaciology, 1-11, 10.1017/jog.2024.29, 2024.

Schoof, C.: The effect of cavitation on glacier sliding, Proceedings of the Royal Society A: Mathematical, Physical and Engineering Science, 461, 609-627, https://doi.org/10.1098/rspa.2004.1350, 2005.

Shepard, M. K., Campbell, B. A., Bulmer, M. H., Farr, T. G., Gaddis, L. R., and Plaut, J. J.: The roughness of natural terrain: A planetary and remote sensing perspective, J. Geophys. Res.-Planets, 106, 32777-32795, 10.1029/2000je001429, 2001.

Van Tricht, L., Huybrechts, P., Van Breedam, J., Furst, J. J., Rybak, O., Satylkanov, R., Ermenbaiev, B., Popovnin, V., Neyns, R., Paice, C. M., and Malz, P.: Measuring and inferring the ice thickness distribution of four glaciers in the Tien Shan, Kyrgyzstan, Journal of Glaciology, 67, 269-286, 10.1017/jog.2020.104, 2021.

Veitch, S. A., Karplus, M., Kaip, G., Gonzalez, L. F., Amundson, J. M., and Bartholomaus, T. C.: Ice thickness estimates of Lemon Creek Glacier, Alaska, from active-source seismic imaging, Journal of Glaciology, 67, 824-832, 10.1017/jog.2021.32, 2021.

Wang, L., Liu, H., Bhlon, R., Chen, D., Long, J., and Sherpa, T. C.: Modeling glacio-hydrological processes in the Himalayas: A review and future perspectives, Geography and Sustainability, 5, 179-192, 10.1016/j.geosus.2024.01.001, 2024.

Wang, P., Li, Z., Li, H., Yao, H., Xu, C., Zhou, P., Jin, S., and Wang, W.: Analyses of recent observations of Urumqi Glacier No. 1, Chinese Tianshan Mountains, Environmental Earth Sciences, 75, 10.1007/s12665-016-5551-3, 2016.

Wang, R.-J., Ding, Y.-J., Shangguan, D.-H., Liu, S.-Y., Guo, W.-Q., Han, H.-D., Li, Y.-J., Song, M., and Zheng, Z.-Q.: Spatial differences of ice volume across High Mountain Asia, Advances in Climate Change Research, 14, 511-521, 10.1016/j.accre.2023.08.004, 2023.

Weertman, J.: On the Sliding of Glaciers, Journal of Glaciology, 3, 33-38, doi:10.3189/S0022143000024709, 1957.

Welty, E., Zemp, M., Navarro, F., Huss, M., Fürst, J. J., Gärtner-Roer, I., Landmann, J., Machguth, H., Naegeli, K., Andreassen, L. M., Farinotti, D., and Li, H.: Worldwide version-controlled database of glacier thickness observations, Earth Syst. Sci. Data, 12, 3039-3055, 10.5194/essd-12-3039-2020, 2020.

Woodard, J. B., Zoet, L. K., Iverson, N. R., and Helanow, C.: Inferring forms of glacier slip laws from estimates of ice-bed separation during glacier slip, Journal of Glaciology, 69, 324-332, 10.1017/jog.2022.63, 2022.

Wu, K., Liu, S., Zhu, Y., Liu, Q., and Jiang, Z.: Dynamics of glacier surface velocity and ice thickness for maritime glaciers in the southeastern Tibetan Plateau, Journal of Hydrology, 590, 125527, https://doi.org/10.1016/j.jhydrol.2020.125527, 2020.

Yao, T., Thompson, L., Yang, W., Yu, W., Gao, Y., Guo, X., Yang, X., Duan, K., Zhao, H., Xu, B., Pu, J., Lu, A., Xiang, Y., Kattel, D. B., and Joswiak, D.: Different glacier status with atmospheric circulations in Tibetan Plateau and surroundings, Nat. Clim. Chang., 2, 663-667, 10.1038/nclimate1580, 2012.

Zekollari, H., Huss, M., Farinotti, D., and Lhermitte, S.: Ice-Dynamical Glacier Evolution Modeling—A Review, Rev. Geophys., 60, 10.1029/2021rg000754, 2022.

https://doi.org/10.5194/egusphere-2025-5838
Preprint. Discussion started: 26 January 2026
© Author(s) 2026. CC BY 4.0 License.

Zoet, L. K. and Iverson, N. R.: A slip law for glaciers on deformable beds, Science, 368, 76-78, doi:10.1126/science.aaz1183, 2020.

Zou, X. J., Gao, H. F., Zhang, Y. S., Ma, N., Wu, J. F., and Bin Farhan, S.: Quantifying ice storage in upper Indus river basin using ground-penetrating radar measurements and glacier bed topography model version 2, Hydrol. Process., 35, 14, 10.1002/hyp.14145, 2021.